Revista de Metalurgia
January–March 2020, 56 (1) e163
ISSN-L: 0034-8570
http://doi.org/10.3989/revmetalm.163

Microstructural properties and tribological behaviours of Ultra-High frequency induction rapid sintered Al-WC composites

Uğur Çavdar[a,*], Levent Ulvi Gezici[b], Burak Gül[b], Mehmet Ayvaz[c]

[a] İzmir Demokrasi University, Engineering Faculty, Mechanical Engineering Department, İDU Campus, 35140, İzmir/Turkey
[b] Celal Bayar University, Engineering Faculty. Department of Mechanical Engineering, 45140 Manisa, Turkey
[c] Vocational School of Manisa Technical Sciences, Manisa Celal Bayar University, Manisa, Turkey
(*Corresponding author: ugur.cavdar@idu.edu.tr)

Submitted: 12 November 2019; Accepted: 20 January 2020; Available On-line: 20 July 2020

ABSTRACT: In this study, sinterability of 1, 3, 5, 9 and 15 wt.% WC reinforced aluminum matrix composite samples by induction fast and conventional sintering methods was investigated. For this purpose, firstly, it was pressed by unaxial cold pressing method under 200 MPa pressure. Some of these raw samples were sintered by ultra-high frequency induction fast sintering method at 600 ºC temperature for 300 sec., while the other part of the samples were sintered by 600 °C for 1800 sec. The density and hardness values of sintered composite samples were measured and microstructural properties, abrasion and friction behaviours were investigated. In this study, it was seen that increased WC reinforcement ratio and abrasion resistance and friction coefficient increased together. In addition, this study showed that ultra-high frequency sintering is as successful as traditional method in Al-WC composite production.

KEYWORDS: Al-WC; Aluminum composite; Friction; Induction sintering; Pin on disc; Wear

Citation/Citar como: Çavdar, U.; Ulvi Gezici, L.; Gül, B.; Ayvaz, M. (2020). "Microstructural properties and tribological behaviours of Ultra-High frequency induction rapid sintered Al-WC composites". *Rev. Metal.* 56(1): e163. https://doi.org/10.3989/revmetalm.163

RESUMEN: *Propiedades microestructurales y comportamiento tribológico de composites Al-WC sinterizados mediante inducción rápida a ultra alta frecuencia.* En este estudio, se analiza la sinterabilidad de composites de matriz de aluminio reforzados con WC 1, 3, 5, 9 y 15% (en peso) y obtenidos por inducción rápida y métodos tradiconales. El procedimiento seguido fue, en primer lugar, presionar mediante un método de prensado en frío no axial con una presión de 200 MPa. Algunas de estas muestras patrones se sinterizaron mediante un método de sinterización por inducción rápida a ultra alta frecuencia, durante 300 s a temperatura de 600 °C. Otras muestras se sinterizaron a 600 °C durante 1800 s. Se midieron los valores de densidad y dureza de los composites sinterizados y se ensayaron las propiedades microestructurales, y el comportamiento de abrasión y de fricción. Se observó que si se aumentaba la relación de refuerzo de WC la resistencia a la abrasión y el coeficiente de fricción tambien aumentaban. Finalmente, el estudio mostró que la sinterización a ultra alta frecuencia es una alternativa tan válida como el método tradicional de obtención de composites de Al-WC.

PALABRAS CLAVE: Al-WC; Composites de aluminio; Desgaste; Fricción; Pin on disc; Sinterización por inducción

ORCID ID: Uğur Çavdar (https://orcid.org/0000-0002-3434-6670); Levent Ulvi Gezici (https://orcid.org/0000-0002-0353-3270); Burak Gül (https://orcid.org/0000-0002-4446-4259); Mehmet Ayvaz (https://orcid.org/0000-0002-9671-8679)

1. INTRODUCTION

Metal matrix composites (MMCs) are developed for optimum combinations of low weight and cost, high strength, abrasion and corrosion resistance. In the production of aluminum metal matrix composites (AMMCs), it is aimed to improve the mechanical properties of the monolytic aluminum alloys, which is the basic material of air, land and sea transportation vehicles due to their low density (Sun and Lei, 2008; Idusuyi and Olayinka, 2019; Imran and Khan, 2019; Panwar and Chauhan, 2018; Krishan *et al*., 2019). The mechanical properties which are intended to be developed are in particular weak creep, fatigue, tensile strength, abrasion and corrosion resistance (Sun and Lei, 2008; He *et al*., 2008; Yandouzi *et al*., 2009; Barbera *et al*., 2016; Roseline and Paramasivam, 2019; Ravindran *et al*., 2019; Giugliano *et al*., 2019). For this purpose, aluminum alloys are reinforced with oxide such as Al_2O_3, SiO_2 and TiO_2, boride such as TiB, nitride such as BN and carbide particles such as B4C, SiC and TiC (Busquets *et al*., 2005; Rodrigo *et al*., 2005; Fernandez *et al*., 2005; Egizabal *et al*., 2010; Gezici *et al*., 2018; Sivakumar *et al*., 2018; Jalilvand *et al*., 2019; Philip *et al*., 2019; Ao *et al*., 2019; Kvashnin *et al*., 2019; Zhou *et al*., 2019; Durmuş *et al*., 2019; Khodabakhshi *et al*., 2019; Shinde *et al*., 2019). One of the popular subjects of recent years is AMMCs, which is used as WC reinforcement as carbide particle (Li *et al*., 2019; Hegde *et al*., 2019; Banerjee *et al*., 2019; Ziejewska *et al*., 2019; Cardoso *et al*., 2019; Gopal Krishna *et al*., 2019).

In their study, Bernoosi *et al.* (2014) produced 1, 3, 5 and 7 wt.% WC reinforced composite samples having Al4.5Cu matrix composition by hot pressing method. Composite powder mixtures were obtained by planetary ball milling method. As a result of the tests carried out, 5 wt.% WC reinforced composite sample was determined as having the highest hardness and yield strength. When the WC reinforcement ratio of 7 wt.% was reached, the hardness and strength of the composite sample decreased.

Pakdel *et al.* (2017) produced nanoscale and micro WC particulate reinforced aluminum matrix composites using the spark plasma method. In the study, 1,5 and 10 wt.% WC was used in both nano and micro composites. In addition, 400, 450 and 500 ^{o}C spark plasma sintering temperatures were used in the study. As a result of the tests performed, it was observed that the sintering temperature had no significant effect on the hardness values of 1wt.% WC reinforced composite samples. However, hardness increased with increasing sintering temperature in 5 and 10% WC reinforced composite samples. In addition, in this study, a decrease in hardness was observed when the reinforcing ratio increased over 5 wt.% in nano WC reinforced composites.

Selvakumar *et al.* (2016) produced 2, 4, 6, 8 and 10 wt.% nano WC reinforced aluminum matrix composites by liquid metallurgy method. As a result of the tests, the Brinell hardness and density values of composite samples were increased and coefficient of friction (COF) and wear losses decreased with increasing WC reinforcement content. Pal *et al.* (2018) produced 1, 1.5 and 2 wt.% WC reinforced aluminum matrix composites with ultrasonic cavitation assisted stir casting method. Similarly, in this study, it has been determined that the wear resistance of composite samples increased with increasing amount of WC reinforcement. Simon *et al.* (2015) produced 5, 10 and 15 wt.% WC reinforced Al matrix composite samples by powder metallurgy method. In this study, the hardness values of composite samples decreased after 5 wt.% WC reinforcement ratio. Wear loss values determined after the wear tests of the samples also increased after 5% WC reinforcement rate, similar to previous studies. In addition, Al_2Cu and $Al_{12}W$ intermetallic phases were determined in the study.

In the production of carbide reinforced aluminum matrix composites, it is desirable to prevent carbon reductions in the reinforcement, oxidation of the matrix and reinforcement, and the formation of intermetallic phases such as Al_4C_3 (Trujillo-Vazquez *et al.*, 2016; Guo *et al.*, 2018; Zhang *et al.*, 2019). To achieve this, the sintering temperature or sintering time must be reduced. Sintering methods in which the sintering time and the temperature of an amount are reduced are called fast sintering methods. Induction, microwave and spark plasma sintering are widely used fast sintering methods (Torralba and Campos, 2014; Sarı Çavdar and Çavdar, 2015; Taştan *et al.*, 2015; Taştan *et al.*, 2019). In the literature, there are studies on Al-WC and Al-WC-Co composite samples sintered by microwave and spark plasma method (Yuying *et al.*, 2010; Ghasali *et al.*, 2015; Pakdel *et al.*, 2017). However, there is no study of Al-WC composites produced using induction sintering which is another fast sintering method. Therefore, in this study, ultra-high frequency induction sinterability of 1, 3, 5, 9 and 15 wt.% WC reinforced composite samples and comparison of produced Al-WC composites with conventional sintering were performed.

2. MATERIALS AND METHODS

In this study, aluminum matrix composite samples with 1, 3, 5, 9 and 15 wt.% WC reinforcing amount sintered using ultra-high frequency induction sintering and conventional sintering methods were produced and microstructural properties and tribological behavior of these composite samples were examined and compared. Both aluminum and WC powders used in the study have high chemical purity (99.8%) and average powder

size of 75 microns. The powder contents of the composite samples were prepared using Acculab precision Weighing Balances with a sensitivity of 0.0001 g. The weighed powders were mixed and ball milled in the AISI 316 stainless steel box at 56 rpm for 30 min. AISI 316 stainless steel balls in a ratio of 1:10 were used to obtain a homogeneous powder mixture. The prepared powder mixtures were pressed with a pressure of 200 MPa in AISI D2 steel mold having a diameter of 16 mm by using unidirectional cold pressing method and green compacts were obtained. Some green samples were sintered at 600 °C for 1800 sec. by conventional method. For conventional sintering process, Protherm laboratory type furnaces with 10 °C min^{-1}. heating rate were used. The other portion of the green samples was sintered using the ultra-high frequency sintering (UHFIS) method at 600 °C for 300 sec. with a heating rate of 100 °C sec^{-1}. In the induction rapid sintering process of green samples, 2.8 kW power and 900 kHz ultra-high frequency induction generator and 20 mm diameter cylindrical coils were used.

The apparent density measurements of the sintered samples were carried out using the Archimedes principle in accordance with ASTM B962-17 (2017) standards. Hardness measurements were carried out by Brinell method in accordance with ASTM E10-18 (2018) standards. For these Brinell hardness measurements, 62.5 kgf and 2.5 mm diameter steel balls were used. Measurements were repeated a minimum of 5 times for each sample and average values were presented. For microstructural examination of samples sintered by sieved by conventional method and UHFIS method, samples were sanded with 100-1200 grid sanders. The surfaces of the sanded samples were polished with 3 and 1 μm diamond polisher, respectively. Keller's reagent - 2ml HF (48%) + 3ml HCl + 5ml HNO_3 + 190ml H_2O were used for etching the sample surfaces. Carl Zeiss 300VP scanning electron microscope (SEM) was used in microstructural examinations in İzmir Katip Çelebi University Central Laboratory.

CSM Instruments tribometer tester was used to examine the tribological properties of aluminum matrix composite samples containing 3, 9 and 15 wt.% WC sintered by UHFIS and traditional methods. The tests were carried out in accordance with ASTM G99-05 standards. Pin-on-disk method was used as abrasion test method. 100Cr6 stainless steel balls with a diameter of 6 mm were used as spherical end pins. In tribological tests carried out at a sliding distance of 100 m, a load of 5N was applied and a shear rate of 10 ms^{-1} was used. As a result of tribological tests, friction coefficients of the samples were determined depending on the sliding distance. Wear properties and regimes of WC reinforced composite samples were determined by SEM.

3. RESULTS AND DISCUSSIONS

The volumes and weight values of WC reinforced composite samples sintered by conventional and UHFIS methods after compaction and after pressing are given in Tables 1 and 2. From these tables, it can be clearly seen that there were shrinkages in both UHFIS and composite samples sintered by conventional method. Due to the nature of the powder metallurgy production process, there are many open pores in the hard particle reinforced composite structure after pressing. These open pores, also found in WC reinforced composites, were somewhat closed after UHFIS and conventional sintering

Table 1. Changes in weight and volume of the conventional sintered Al-WC composite samples

	After Pressing		After Sintering			
WC (wt.%)	Weight (g)	Volume (cm^3)	Weight (g)	Weight Change (%)	Volume (cm^3)	Volume Change (%)
1	1.9919	0.7984	1.9956	0.185	0.7902	-1.020
3	1.9908	0.8147	1.9918	0.050	0.7902	-3.0
5	1.9919	0.8106	1.9927	0.040	0.7882	-2.763
9	1.9927	0.8126	1.9981	0.270	0.7902	-2756
15	1.9893	0.7984	1.9917	0.120	0.7861	-1.530

Table 2. Changes in weight and volume of the ultra-high frequency induction sintered Al-WC composite samples

	After Pressing		After Sintering			
WC (wt.%)	Weight (g)	Volume (cm^3)	Weight (g)	Weight Change (%)	Volume (cm^3)	Volume Change (%)
1	1.9933	0.7973	1.9939	0.030	0.7943	-0.379
3	1.9909	0.8147	1.9905	-0.020	0.7902	-3
5	1.9954	0.8126	1.9949	-0.025	0.7902	-2.756
9	2.0063	0.8024	2.0058	-0.024	0.7923	-1.269
15	1.9993	0.8024	1.9990	-0.015	0.7678	-4.314

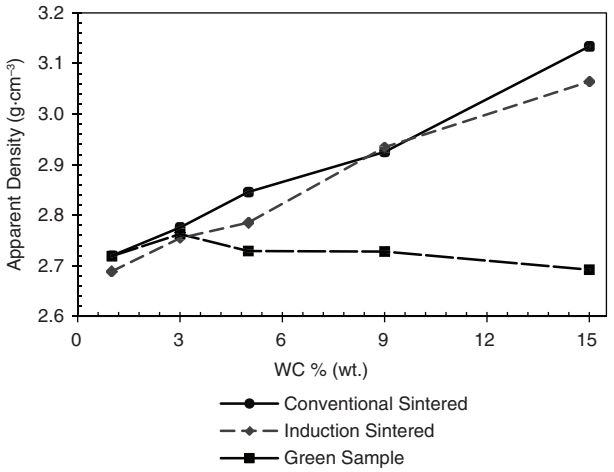

FIGURE 1. The variation of apparent density values of green, induction and conventional sintered composite samples depending on WC ratio.

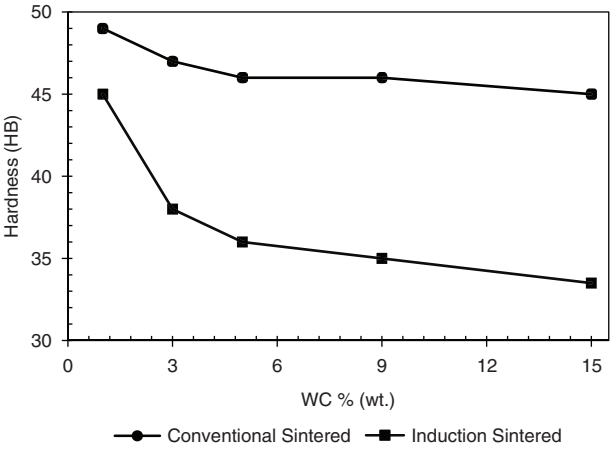

FIGURE 2. The variation of Brinell hardness values of induction and conventional sintered composite samples depending on WC ratio.

processes, and shrinkage occurred in composite samples. When the weight changes after sintering are examined, it is seen that the weight of composite samples sintered by UHFIS process was generally decreased. On the other hand, there was an increase in weight of all sintered samples by conventional method. In conventional sintered samples, the aluminum matrix was oxidized by sintering in an open atmosphere, thus increasing the weight of the composite samples. The weight was reduced due to less oxidation of the fast sintered samples by the UHFIS method and the evaporation of the mold lubricant that had penetrated into the composite sample during pressing. Similarly, in previous studies, it was found that aluminum oxide thickness increased gradually with increasing process time (Baran *et al.*, 2014).

The apparent density values of green compacts and composites sintered by conventional and UHFIS methods depending on the amount of WC reinforcement are given in Fig. 1. In green samples, there was some increase in apparent density when WC amount increased from 1 to 3 wt.%, but after this point, apparent density decreased with increasing WC amount. This was due to the reduced compressibility of the composite material due to the increased amount of WC, thereby increasing the amount of porosity. After sintering, similar to literature, the apparent densities of the composite samples increased with the decrease of open pores (Simon *et al.*, 2015). This increase was parallel to the increase in the amount of WC. Figure 2 shows the Brinell hardness of the composite samples sintered by UHFIS and conventional sintering methods. The Brinell hardness of composite samples decreased with increasing amount of WC. This is due to the fact that WC particles reduce the sinterability of the composite sample. Furthermore, it is seen that this decrease occurs more sharply in the induction fast sintered composite sample.

The SEM micrographs of microstructures of conventional and UHFIS sintered, 1, 3, 5, 9 and 15 wt.% WC reinforced aluminum matrix composite samples are given in Figs. 3 and 4, respectively. In the SEM micrographs, the grey area is Aluminum metal matrix, the white areas are WC particles and the black areas are open pores. When the SEM micrographs are examined, it can be seen that a homogeneous WC distribution is obtained in all samples. In addition, there is no apparent difference in the amount of porosity between the composite samples sintered by conventional and UHFIS methods. However, as shown in Fig. 5, intermetallic compounds having a needle-like structure were observed in the samples sintered by the UHFIS process. As an interesting and important data, in the EDS analysis obtained from this intermetallic phase formed by electromagnetic induction current as short as 300 seconds, this compound was found to be Al-Fe compound. The Al-Fe intermetallic phase formation has been observed in the literature in powder metallurgy method (Wang *et al.*, 1998; Fathy *et al.*, 2015).

The coefficients of friction of 3, 9 and 15 wt.% WC reinforced Al matrix composites sintered by conventional and UHFIS methods can be seen in Figs. 6 and 7, respectively. The point where the friction coefficient line makes the first peak is the coefficient of static friction of that sample. After this point, it gives the kinetic friction coefficient of the composite material. In general, friction coefficient values are parallel to the data in the literature (Selvakumar *et al.*, 2016; Pal *et al.*, 2018; Li *et al.*,

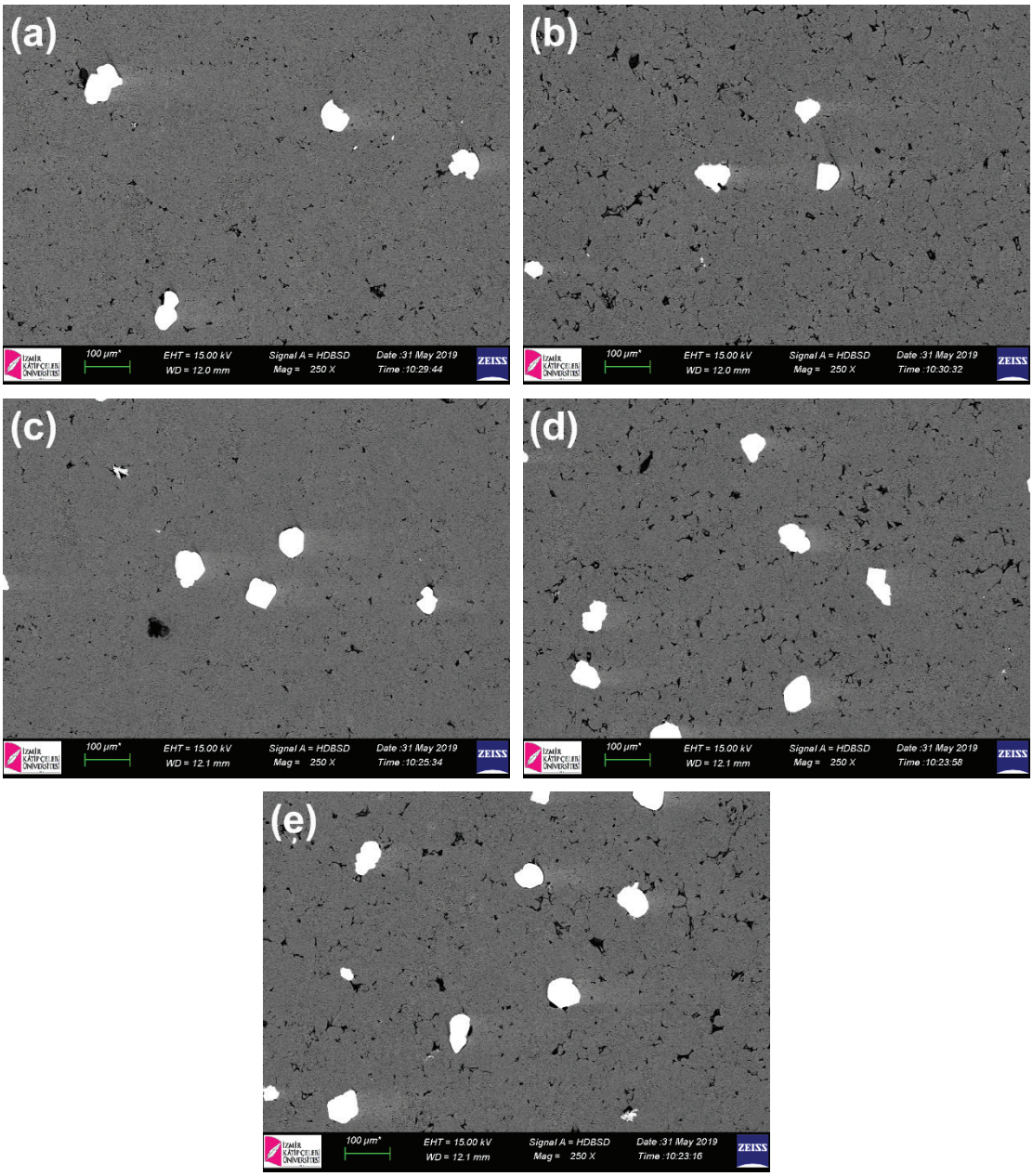

FIGURE 3. The SEM micrographs of the microstructures of conventional sintered composite samples: (a) 1, (b) 3, (c) 5, (d) 9 and (e) 15 wt. % WC reinforced composites.

2019). When the graphs are analyzed, it is seen that 15 wt. % WC reinforced composite sample has the highest coefficient of both static and kinetic friction. There was no significant change in the mean friction coefficients of 9 and 15 wt.% WC reinforced composite samples sintered by conventional and induction sintering method. However, with induction sintering, it was found that the average coefficient of friction of 3 wt.% WC reinforced composite sample decreased and the coefficients of friction of composite samples sintered by UHFIS method increased in parallel with increase in the amount of WC.

The SEM micrographs of the corroded surfaces of 3, 9 and 15 wt.% WC reinforced aluminum matrix composites sintered by conventional and UHFIS methods are shown in Fig. 8, respectively. When the micrographs of the worn surfaces are examined, it is seen that the dominant wear type was delamination in the sintered composites by

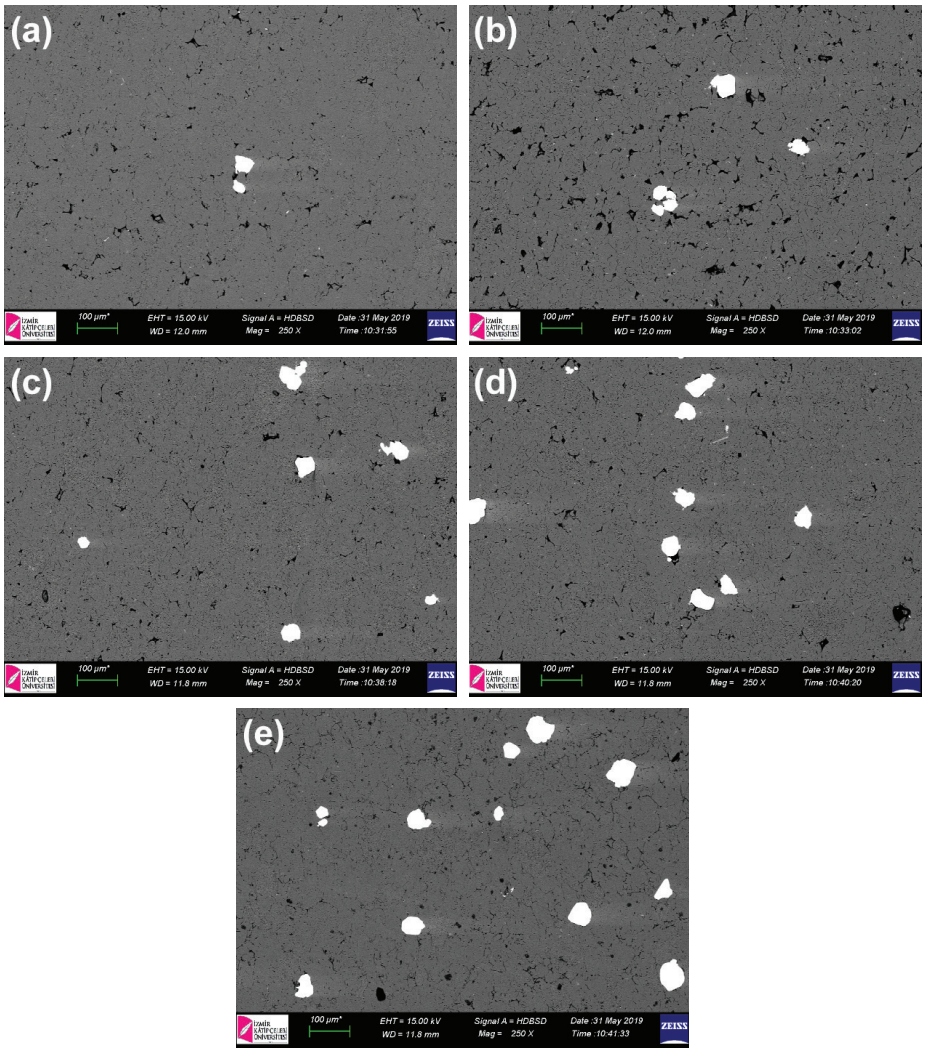

FIGURE 4. The SEM micrographs of the microstructures of induction sintered composite samples: (a) 1, (b) 3, (c) 5, (d) 9 and (e) 15 wt.% WC reinforced composites.

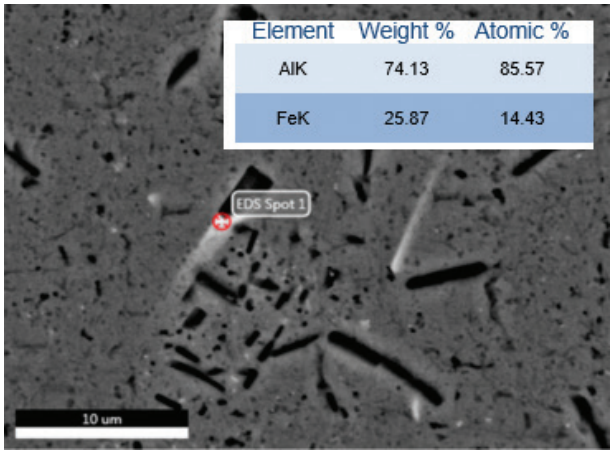

FIGURE 5. The SEM-EDS analysis from 5 wt.% WC reinforced induction sintered composite sample.

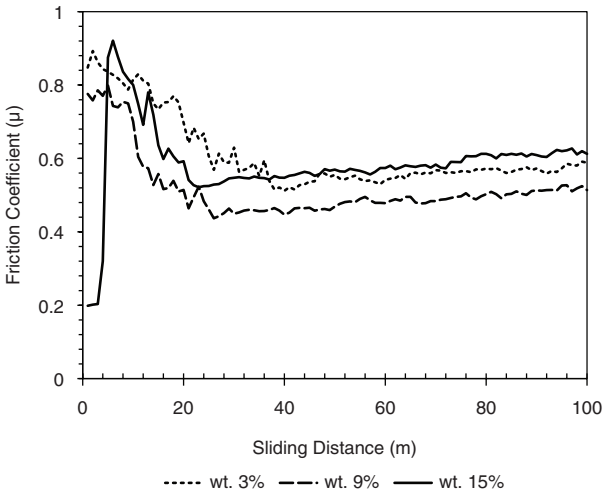

FIGURE 6. The variation in friction coefficients of conventional sintered composite samples as a function of sliding distance.

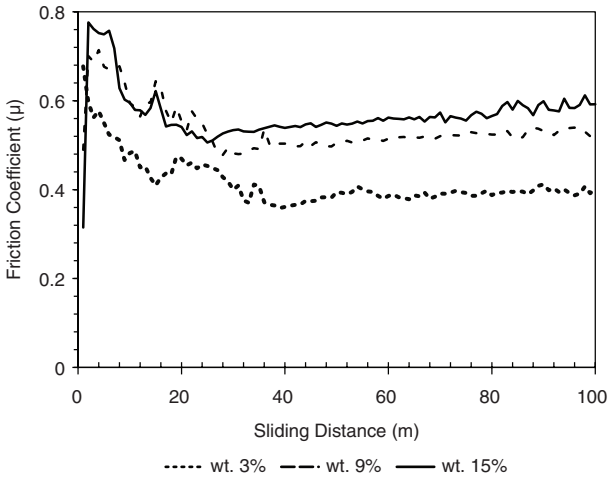

FIGURE 7. The variation in friction coefficients of induction sintered composite samples as a function of sliding distance

traditional method. On the other hand, abrasive type wear as a dominant wear regime was observed in UHFIS method. This is understood from the flaking off and plastic deformation zones of the samples sintered by the conventional method and the deep abrasive grooves on the surfaces of the sample sintered by the UHFIS method. Of all composite samples, the largest wear scar was seen in the 3 wt.% WC reinforced composite sample sintered by the conventional method. In composite samples sintered by UHFIS method, wear scar width decreased with increasing amount of WC reinforcement and the narrowest wearing scar was determined in 15 wt.% WC reinforced sample sintered by UHFIS method in all composite samples. SEM investigations of worn surfaces generally show that composite samples sintered by the UHFIS method have a higher wear resistance than conventional sintered samples.

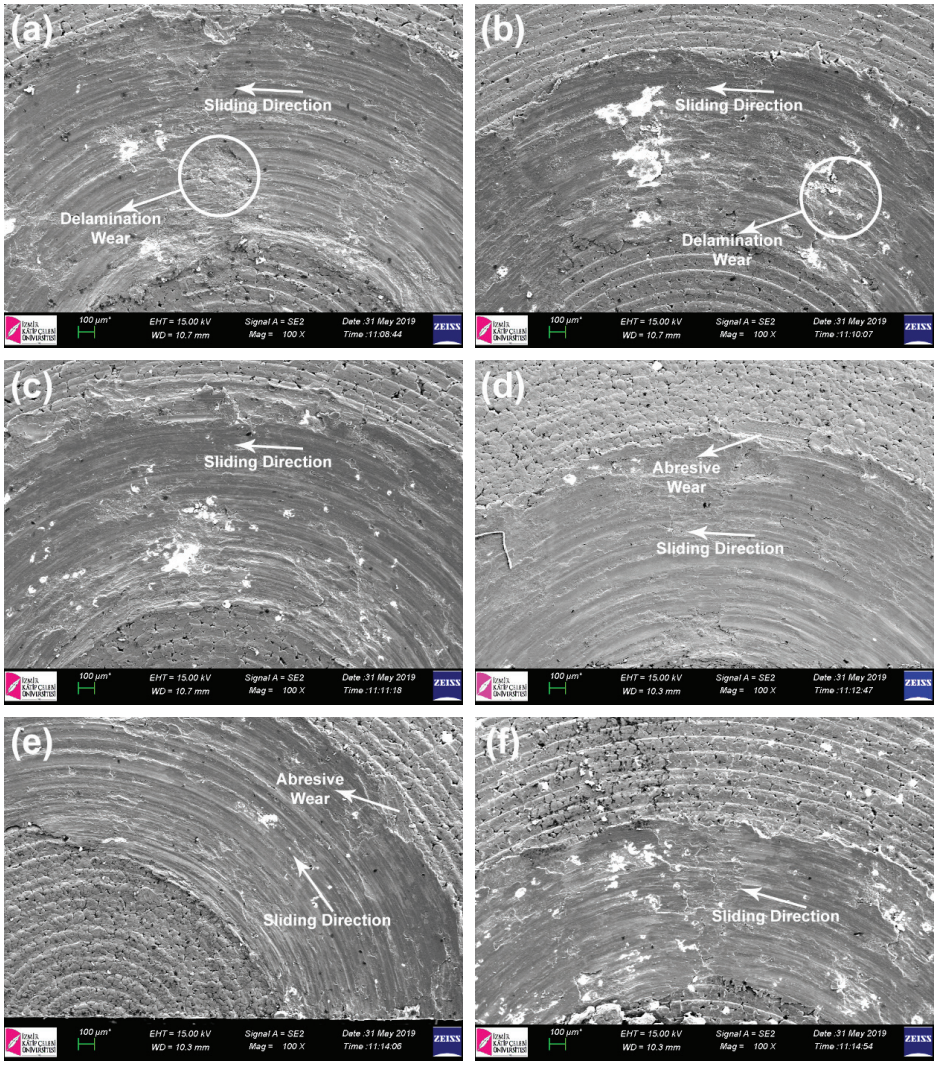

FIGURE 8. The SEM images of worn surfaces of composite samples: (a) 3, (b) 9, (c) 15 wt.% WC reinforced traditional sintered composites, (d) 3, (e) 9, (f) 15 wt.% WC reinforced induction sintered composite samples.

4. CONCLUSIONS

In this study, sinterability, microstructure, wear and friction behavior of composite samples containing 1, 3, 5, 9 and 15 wt.% WC sintered at 600 ºC, 1800 sec conventional method and 300 sec UHFIS method were investigated. The results can be listed as follows:

- In the sintered samples by the conventional method, the weight increase after the sintering is determined, while the weight of the induction sintered samples decreases. The increase in weight in samples sintered by the conventional method is due to oxidation.
- In composite samples sintered both by the conventional method and the UHFIS method, the apparent density increases as the WC reinforcement content increases.
- The Brinell hardness of samples, both conventional and UHFIS methods sintering, WC reinforcement content increases as hardness decreases.
- The Al-Fe intermetallic phase formation was realized in composite samples sintered by UHFIS method.
- Among the composite samples sintered by both conventional and UHFIS methods, 15 wt.% WC reinforced composite samples have the highest coefficient of static and kinetic friction values. The narrowest wear track width was also determined in these samples.

REFERENCES

Ao, M., Liu, H., Dong, C. (2019). The effect of La_2O_3 addition on intermetallic-free aluminium matrix composites reinforced with TiC and Al_2O_3 ceramic particles. *Ceram. Int.* 45 (9), 12001–12009. https://doi.org/10.1016/j.ceramint.2019.03.093.

ASTM B962 (2017). Standard Test Methods for Density of Compacted or Sintered Powder Metallurgy (PM) Products Using Archimedes' Principle. ASTM International, West Conshohocken, PA.

ASTM E10-18 (2018). Standard Test Method for Brinell Hardness of Metallic Materials. ASTM International, West Conshohocken, PA.

Banerjee, S., Poria, S., Sutradhar, G., Sahoo, P. (2019). Dry sliding tribological behavior of AZ31-WC nano-composites. *J. Magnesium Alloys* 7 (2), 315–327. https://doi.org/10.1016/j.jma.2018.11.005.

Baran, J.D., Grönbeck, H., Hellman, A. (2014). Mechanism for limiting thickness of thin oxide films on aluminum. *Phys. Rev. Lett.* 112 (14), 1–5. https://doi.org/10.1103/PhysRevLett.112.146103.

Barbera, D., Chen, H., Liu, Y. (2016). Creep-fatigue behaviour of aluminum alloy-based metal matrix composite. *Int. J. Press. Vessels Pip*. 139–140, 159–172. https://doi.org/10.1016/j.ijpvp.2016.02.004.

Bernoosi, S., Khosroshahi, R.A., Mousavian, R.T. (2014). Mechanical properties of hot-pressed Al-4.5 wt. % Cu/WC composite. *JUFGNSM* 47 (2), 63–70. https://doi.org/10.7508/jufgnsm.2014.02.002.

Busquets, D., Gomez, L., Amigó, V., Salvador-Moya, M.D. (2005). Study of mechanical properties on powdermetalurgy aluminium matrix composites fabricated by stamping or extrusion. *Rev. Metal.* 41 (5), 365–373. https://doi.org/10.3989/revmetalm.2005.v41.i5.226.

Cardoso, J.P., Puga, J., Ferro Rocha, A.M., Fernandes, C.M., Senos, A.M.R. (2019). WC – (Cu: AISI304) composites processed from high energy ball milled powders. *Int. J. Refract. Met. Hard Mater*. 84, 1–8. https://doi.org/10.1016/j.ijrmhm.2019.104990.

Durmuş, H., Gül, C., Çömez, N., Yurddaşkal, M. (2019). An investigation into the wear behavior of aged Alumix321/SiC composites fabricated by hot pressing. *Rev. Metal.* 55 (3), e148. https://doi.org/10.3989/revmetalm.148.

Egizabal, P., Merchan, M., Garcia-de-Cortazar, M., Plaza, L.M., Torregaray, A. (2010). Development and characterization of a metal matrix composite of aluminium 6061 and TiB_2 particulates. *Rev. Metal.* 46 (Nº Extra), 128–132. https://doi.org/10.3989/revmetalmadrid.13XIIPMS.

Fathy, A., El-Kady, O., Mohammed, M.M.M. (2015). Effect of iron addition on microstructure, mechanical and magnetic properties of Al-matrix composite produced by powder metallurgy route. *Trans. Nonferrous Met. Soc. China* 25 (1), 46–53. https://doi.org/10.1016/S1003-6326(15)63577-4.

Fernandez, R., Garcia-Alonso, E., Gonzales-Doncel, G. (2005). Creep behavior of a PM Al6061-15 vol % SiC_w metal matrix composite. *Rev. Metal.* 41 (Nº Extra), 239–243, https://doi.org/10.3989/revmetalm.2005.v41.iExtra.1032.

Gezici, L.U., Gül, B., Çavdar, U. (2018). The mechanical and tribological characteristics of aluminum-titanium dioxide composite. *Rev. Metal.* 54 (2), e119. https://doi.org/10.3989/revmetalm.119.

Ghasali, E., Pakseresht, A.H., Agheli, M., Marzbanpour, H., Ebadzadeh, T. (2015). WC-Co particles reinforced aluminum matrix by conventional and microwave sintering. *Mater. Res*. 18 (6), 1197–1202. http://dx.doi.org/10.1590/1516-1439.027115.

Giugliano, D., Barbera, D., Chen, H., Cho, N.K., Liu, Y. (2019). Creep-fatigue and cyclically enhanced creep mechanisms in aluminium based metal matrix composites. *Eur. J. Mech. A. Solids* 74, 66–80. https://doi.org/10.1016/j.euromechsol.2018.10.015.

Gopal Krishna, U.B., Ranganatha, P., Rajesh, G.L., Auradi, V., Mahendra Kumar, S., Vasudeva, B. (2019). Studies on dry sliding wear characteristics of cermet WC-Co particulate reinforced Al7075 metal matrix composite. *Proceedings: Materials Today,* Vol. 16 (Part.2), 343–350. https://doi.org/10.1016/j.matpr.2019.05.100.

Guo, B., Chen, B., Zhang, X., Cen, X., Wang, X., Song, M., Ni, S., Yi, J., Shen, T., Du, Y. (2018). Exploring the size effects of Al_4C_3 on the mechanical properties and thermal behaviors of Al-based composites reinforced by SiC and carbon nanotubes. *Carbon* 135, 224–235. https://doi.org/10.1016/j.carbon.2018.04.048.

He, C., Zhou, Q., Liu, J., Geng, X., Cai, Q. (2008). Effect of size of reinforcement on thickness of anodized coatings on SiC/Al matrix composites. *Mater. Lett.* 62 (16), 2441–2443. https://doi.org/10.1016/j.matlet.2007.12.016.

Hegde, N.T., Pai, D., Hegde, R. (2019). Heat treatment and mechanical characterization of LM-25/tungsten carbide metal matrix composites. *Proceedings: Materials Today,* Vol. 19 (Part. 2), 810–817. https://doi.org/10.1016/j.matpr.2019.08.136.

Idusuyi, N., Olayinka, J.I. (2019). Dry sliding wear characteristics of aluminum metal matrix composites: abrief overview. *J. Mater. Res. Technol*. 8 (3), 3338–3346. https://doi.org/10.1016/j.jmrt.2019.04.017.

Imran, M., Khan, A.R.A. (2019). Characterization of Al-7075 metal matrix composite: a review. *J. Mater. Res. Technol*. 8 (3), 3347–3356. https://doi.org/10.1016/j.jmrt.2017.10.012.

Jalilvand, M.M., Mazaheri, Y., Heidarpour, A., Roknian, M. (2019). Development of A356/Al_2O_3+SiO_2 surface hybrid nanocomposite by friction stir processing. *Surf. Coat. Technol.* 360, 121–132. https://doi.org/10.1016/j.surfcoat.2018.12.126.

Khodabakshi, F., Gerlich, A.P., Verma, D., Haghshenas, M. (2019). Nano-indentation behavior of layered ultra-fine grained AA8006 aluminum alloy and AA8006-B_4C

nanostructured nanocomposite produced by accumulative fold forging process. *Mat. Sci. Eng. A*. 744, 120–136. https://doi.org/10.1016/j.msea.2018.12.013.

Krishan, P.K., Christy, J.V., Arunachalam, R., Mourad, A.-H. I., Muraliraja, R., Al-Maharabi, M., Murali, V., Chandra, M.M. (2019). Production of aluminum alloy-based metal matrix composites using scrap aluminum alloy and waste materials: Influence on microstructure and mechanical properties. *J. Alloys Compd*. 748, 1047–1061. https://doi.org/10.1016/j.jallcom.2019.01.115.

Kvashnin, D.G., Firestein, K.L., Popov, Z.I., Corthay, S., Sorokin, P.B., Golberg, D.V., Shtansky, D.V. (2019). Al - BN interaction in a high-strength lightweight Al/BN metal-matrix composite: Theoretical modelling and experimental verification. *J. Alloys Compd.* 782, 875–880. https://doi.org/10.1016/j.jallcom.2018.12.261.

Li, C., Li, S., Liu, C., Zhang, Y., Deng, P., Guo, Y., Wang, J., Wang, Y. (2019). Effect of WC addition on microstructure and tribological properties of bimodal aluminum composite coatings fabricated by laser surface alloying. *Mater. Chem. Phys.* 234, 9–15. https://doi.org/10.1016/j.matchemphys.2019.05.089.

Pakdel, A., Witecka, A., Rydzek, G., Shri, D.N.A. (2017). A comprehensive microstructural analysis of Al–WC micro- and nano-composites prepared by spark plasma sintering. *Mater. Design* 119, 225–234. https://doi.org/10.1016/j.matdes.2017.01.064.

Pal, A., Poria, S., Sutradhar, G., Sahoo, P. (2018). Tribological behavior of Al-WC nano-composites fabricated by ultrasonic cavitation assisted stir-cast method. *Mater. Res. Express*. 5 (3), 1–16. https://doi.org/10.1088/2053-1591/aab577.

Panwar N., Chauhan, A. (2018). Fabrication methods of particulate reinforced aluminum metal matrix composite-a review. *Proceedings Materials Today* 5 (2), 5933–5939. https://doi.org/10.1016/j.matpr.2017.12.194.

Philip, S.V., Selvam, J.D.R., Rajakumar, S.R., Mashninini, P.M. (2019). Microstructure Characterization of in-situ formed Al_2O_3-TiB_2 AMCs particles on AA6061 aluminium matrix composites. *Proceedings Materials Today* 16 (2), 574–578. https://doi.org/10.1016/j.matpr.2019.05.130.

Ravindran, S., Mani, N., Balaji, S., Abhijith, M., Surendaran, K. (2019). Mechanical behaviour of aluminium hybrid metal matrix composite-A review. *Proceedings Materials Today* 16 (2), 1020–1033. https://doi.org/10.1016/j.matpr.2019.05.191.

Rodrigo, P., Poza, P., Utrilla, M.V., Ureña, A. (2005). Effect of ageing on the mechanical behaviour of aluminium alloy AA2009 reinforced with SiC particles. *Rev. Metal.* 41 (4), 298–307. https://doi.org/10.3989/revmetalm.2005.v41.i4.218.

Roseline, S., Paramisav, V. (2019). Corrosion behaviour of heat treated aluminum metal matrix composites reinforced with fused zirconia alumina 40. *J. Alloys Compd.* 799, 205–215. https://doi.org/10.1016/j.jallcom.2019.05.185.

Sarı Çavdar, P., Çavdar, U. (2015). The evaluation of different environments in ultra-high frequency induction sintered powder metal compacts. *Rev. Metal*. 51 (1), e36. https://doi.org/10.3989/revmetalm.036.

Selvakumar, N., Gnanasundaajayaraja, B., Rajeshkumar, P. (2016). Enhancing the properties of Al–WC nanocomposites using liquid metallurgy. *Exp. Tech*. 40, 129–135. https://doi.org/10.1007/s40799-016-0015-y.

Shinde, D.M., Poria, S., Sahoo, P. (2019). Synthesis and characterization of Al-B_4C nano composites. *Proceedings Materials Today* 19 (2), 170–176. https://doi.org/10.1016/j.matpr.2019.06.641.

Simon, A., Lipusz, D., Baumli, P., Balint, P., Kaptay, G., Gergely, G., Sfikas, A., Lekatou, A., Karantzalis, A., Gacsi, Z. (2015). Microstructure and mechanical properties of Al-WC composites. *Arch. Metall. Mater.* 60 (2), 389–393. https://doi.org/10.1515/amm-2015-0164.

Sivakumar, S., Thimmappa, S.K., Golla, B.R. (2018). Corrosion behavior of extremely hard Al-Cu/Mg-SiC light metal alloy composites. *J. Alloys Compd.* 767, 703–711. https://doi.org/10.1016/j.jallcom.2018.07.117.

Sun, R., Lei, Y. (2008). Microstructure and hardness of laser clad SiCp-Al composite coatings on Al alloys. *Mater. Lett.* 62 (17–18), 3272–3275. https://doi.org/10.1016/j.matlet.2008.02.041.

Taştan, M., Gökozan, H., Taşkın, S., Çavdar, U. (2015). Comparative energy consumption analyses of an ultra high frequency induction heating system for material processing applications. *Rev. Metal*. 51 (3), e46. https://doi.org/10.3989/revmetalm.046.

Taştan, M., Gökozan, H., Sarı Çavdar, P., Soy, G., Çavdar, U. (2019). Analysis of artificial aging with induction and energy costs of 6082 Al and 7075 Al materials. *Rev. Metal*. 55 (1), e137. https://doi.org/10.3989/revmetalm.137.

Torralba, J.M., Campos, M. (2014). Towards high performance in powder metallurgy. *Rev. Metal*. 50 (2), e017. https://doi.org/10.3989/revmetalm.017.

Trujillo-Vazquez, E., Pech-Canul, M.I., Guia-Tello, J.C., Pech-Canul, M.A. (2016). Surface chemistry modification for elimination of hydrophilic Al_4C_3 in B_4C/Al composites. *Mater. Design* 89, 94–101. https://doi.org/10.1016/j.matdes.2015.09.149.

Wang, X., Wood, J.V., Sui, Y., Lu, H. (1998). Formation of intermetallic compound in iron-aluminum alloys. *J. of Shanghai Univ.* 2, 305–310. https://doi.org/10.1007/s11741-998-0045-5.

Yandouzi, M., Richer, P., Jodoin, B. (2009). SiC particulate reinforced Al-12Si alloy composite coatings produced by the pulsed gas dynamic spray process: Microstructure and properties. *Surf. Coat. Tech.* 203 (20–21), 3260–3270. https://doi.org/10.1016/j.surfcoat.2009.04.001.

Yuying, W., Xiangfa, L., Guolong, M., Chong, L., Junqing, Z. (2010). High energy milling method to prepare Al/WC composite coatings in Al–Si alloys. *J. Alloys Compd*. 497 (1–2), 139–141. https://doi.org/10.1016/j.jallcom.2010.03.086.

Zhang, W.Y., Du, Y.H., Zhang, P., Wang, Y.J. (2019). Air-isolated stir casting of homogeneous Al-SiC composite with no air entrapment and Al_4C_3. *J. Mater. Process Tech.* 271, 226–236. https://doi.org/10.1016/j.jmatprotec.2019.04.001.

Zhou, Y., Wen, S., Wang, C., Duan, L., Wei, Q., Shi, Y. (2019). Effect of TiC content on the Al-15Si alloy processed by selective laser melting: Microstructure and mechanical properties. *Opt. Laser Technol.* 120, 1–8. https://doi.org/10.1016/j.optlastec.2019.105719.

Ziejewska, C., Marczyk, J., Szewczyk-Nykiel, A., Nykiel, M., Hebda, M. (2019). Influence of size and volume share of WC particles on the properties of sintered metal matrix composites. *Adv. Powder Technol*. 30 (4), 835–842. https://doi.org/10.1016/j.apt.2019.01.013.